Supplementary Material for

Spatial Patterns of Temperature and Precipitation Extremes Across Spain Under Climate Change: A Comparison of Bayesian Approaches

Soledad Collazo[1], David Barriopedro[2], Ricardo García-Herrera[1,2], José Agustín García[3], Santiago Beguería[4], Juan Emmanuel Johnson[5], Sergio M. Vicente-Serrano[6]

[1]Departamento de Física de la Tierra y Astrofísica, Facultad de Ciencias Físicas, Universidad Complutense de Madrid, Madrid, 28040, Spain
[2]Instituto de Geociencias (IGEO), Consejo Superior de Investigaciones Científicas– Universidad Complutense de Madrid, Madrid, Spain
[3]Departamento de Física, Universidad de Extremadura, Badajoz, Spain
[4]Estación Experimental de Aula Dei-Consejo Superior de Investigaciones Cientificas (EEAD-CSIC), Zaragoza, Spain
[5]International Methane Emissions Observatory, Mitigation Branch–Climate Change Division, United Nations Environment Programme, Paris, France
[6]Instituto Pirenaico de Ecología, Consejo Superior de Investigaciones Científicas (IPE- CSIC), Zaragoza, Spain

Correspondence to: Soledad Collazo (scollazo@ucm.es)

Supplementary Text

S1. Bayes' theorem and the hierarchical model structure

Bayesian inference updates prior beliefs about the model parameters θusing the observed data y through Bayes' theorem (Gelman et al. 2013):

$$p(\theta \mid y) \propto p(y \mid \theta)\, p(\theta) \qquad (S1)$$

where $p(y \mid \theta)$ is the GEVD likelihood, $p(\theta)$the prior distribution, and θ the full vector of unknown parameters in the model.

The spatial models used here are hierarchical, with three levels (García et al. 2024):

Data level. Each observation follows a GEVD with parameters that vary by location and time (Eq. 1):

$$y(s,t) \sim \text{GEVD}(\mu(s,t), \sigma(s,t), \xi)$$

Process level. The GEVD parameters depend on geographic covariates, a spatially correlated random effect, and a station-level random term (Eqs. 3–5). For each parameter $k \in \{\mu_0, \mu_1, \sigma_0, \sigma_1\}$:

$$k(s) = x(s) \cdot \alpha_k + W_k(s) + \epsilon_k(s), \qquad \epsilon_k(s) \sim N(0, \tau_k^2) \qquad \text{(S2)}$$

$$W_k(s) \sim \text{MVN}(0, \Sigma_k), \qquad \Sigma_k(s_i, s_j) = \beta_{k_1}^2 \exp\left(-\frac{\| s_i - s_j \|}{\beta_{k_2}}\right)$$

Here $\epsilon_k(s)$is an independent, station-level (nugget) term with variance τ_k^2, representing fine-scale variability not captured by the smooth spatial process $W_k(s)$. Equivalently, conditional on W_k, each parameter is normally distributed:

$$k(s) \mid W_k(s) \;\sim\; N(x(s) \cdot \alpha_k + W_k(s),\, \tau_k^2) \qquad \text{(S3)}$$

Prior level. Weakly informative priors are placed on the regression coefficients α_k, the covariance parameters β_{k_1}, β_{k_2}, the nugget variances τ_k^2, and the shape parameter ξ.

Joint posterior. Combining the three levels, the full posterior distribution is:

$$p(\alpha, W, \beta, \tau, \xi \mid y) \propto \underbrace{\prod_{s,t} \mathrm{GEVD}(y(s,t) \mid \mu(s,t), \sigma(s,t), \xi)}_{\text{likelihood}} \times \underbrace{\prod_k \prod_s P(k(s) \mid x(s), \alpha_k, W_k(s), \tau_k^2)}_{\text{process level}} \times \underbrace{\prod_k \mathrm{P}(W_k \mid \beta_k)}_{\text{spatial random effects}} \times \underbrace{P(\alpha)\, P(\beta)\, P(\tau)\, P(\xi)}_{\text{priors}} \qquad \text{(S4)}$$

so that the spatial random effects W_k, the regression coefficients α_k, the covariance parameters β_k, and the nugget variances τ_k^2 are all estimated jointly, with uncertainty at each level propagating to the others and ultimately to derived quantities such as return levels (Eq. 6).

S2. Prediction at unobserved locations — fully spatial model

For each posterior draw, the spatial effect at unobserved locations was predicted from the spatial effect estimated at the observed stations (Rasmussen and Williams, 2006), using the exponential covariance function of Eq. (5) to weight the contribution of each station according to its distance from the new location. This predicted spatial effect was then combined with the geographic-covariate term of Eq. (3) to obtain the parameter value at the new location. Repeating this procedure across posterior draws propagated uncertainty in the fitted parameters and spatial effects.at each unobserved location. The shape parameter, treated as spatially homogeneous, was applied directly without a separate spatial prediction step.

S3. Prediction at unobserved locations — universal kriging

Under the two-stage approach (Section 3.4), the GEVD parameters are first estimated locally and independently at each station, and the spatial structure of each parameter is then described with universal kriging (Matheron, 2019). The same geographic covariates used in the fully spatial model are included: elevation, latitude, longitude and distance to the coast. The location parameters (μ_0, μ_1) are interpolated directly, and the scale parameter is interpolated on the log scale (log σ) so that it stays positive.

For each parameter, we first build an empirical semivariogram from the posterior median at each station, after removing the part explained by the covariates. The semivariogram shows how the difference between two stations' values grows with the distance between them. Nearby stations with similar values give low semivariance, and distant or dissimilar stations give higher semivariance. We fit an exponential model to each empirical semivariogram by weighted least squares, which gives three quantities:

- the **nugget**, the small-scale or unexplained variability between very close stations;
- the **partial sill**, the size of the spatially structured variation;
- the **range**, the distance beyond which stations are effectively uncorrelated.

Universal kriging at an unobserved location s_0 is then estimated from Eq. S5

$$\hat{k}(s_0) = x(s_0) \cdot \hat{\alpha}_k + \gamma_0^T \Gamma^{-1}(k(s_{1:n}) - \mathbb{X} \cdot \hat{\alpha}_k) \qquad \text{(S5)}$$

where $\hat{\alpha}_k$ are the regression coefficients relating the parameter to the geographic covariates (estimated from the observed stations), X is the matrix of covariates at the observed stations, Γ is the covariance matrix among stations implied by the fitted semivariogram, and γ_0 is the vector of covariances between s_0 and each station.

The semivariogram is fitted only once per parameter, but Eq. S5 is applied separately to every posterior draw, not just to the posterior mean. This carries the uncertainty of the local estimates through the interpolation and gives a full predictive distribution of each parameter at each unobserved location. To keep ξ spatially homogeneous, as assumed in the fully spatial model, the shape parameter is not kriged. Instead, it is pooled across stations into a single value per posterior draw, taken as the median of one randomly sampled draw from each station.

References

García, J. A., Acero, F. J., Martínez-Pizarro, M., and Lara, M.: A Bayesian hierarchical spatio-temporal model for summer extreme temperatures in Spain, Stoch. Environ. Res. Risk Assess., 38, 3393–3410, https://doi.org/10.1007/s00477-024-02754-8, 2024.

Gelman, A., Carlin, J. B., Stern, H. S., Dunson, D. B., Vehtari, A., and Rubin, D. B.: Bayesian Data Analysis, 3rd edn., Chapman and Hall/CRC, Boca Raton, Florida, https://doi.org/10.1201/b16018, 2013.

Matheron, G.: Universal kriging, in: Matheron's Theory of Regionalised Variables, edited by: Pawlowsky-Glahn, V. and Serra, J., Oxford University Press, 123–180, https://doi.org/10.1093/oso/9780198835660.003.0005, 2019.

Rasmussen, C. E. and Williams, C. K. I.: Gaussian Processes for Machine Learning, MIT Press, Cambridge, Massachusetts, https://gaussianprocess.org/gpml/, 2006.

Supplementary Figures

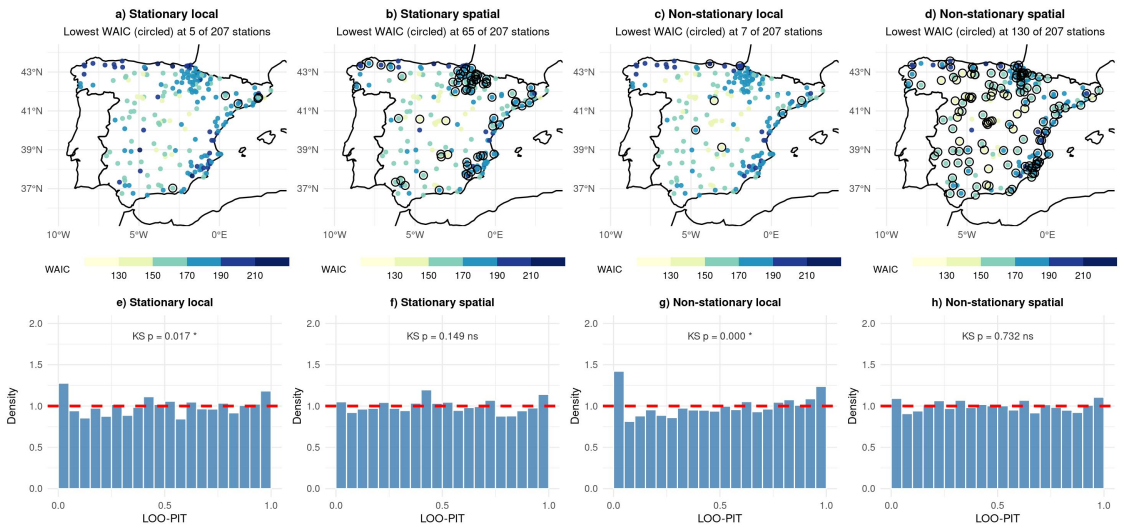


Figure S1: Same as Fig. 2 of the main text but for the Laplace approximation.

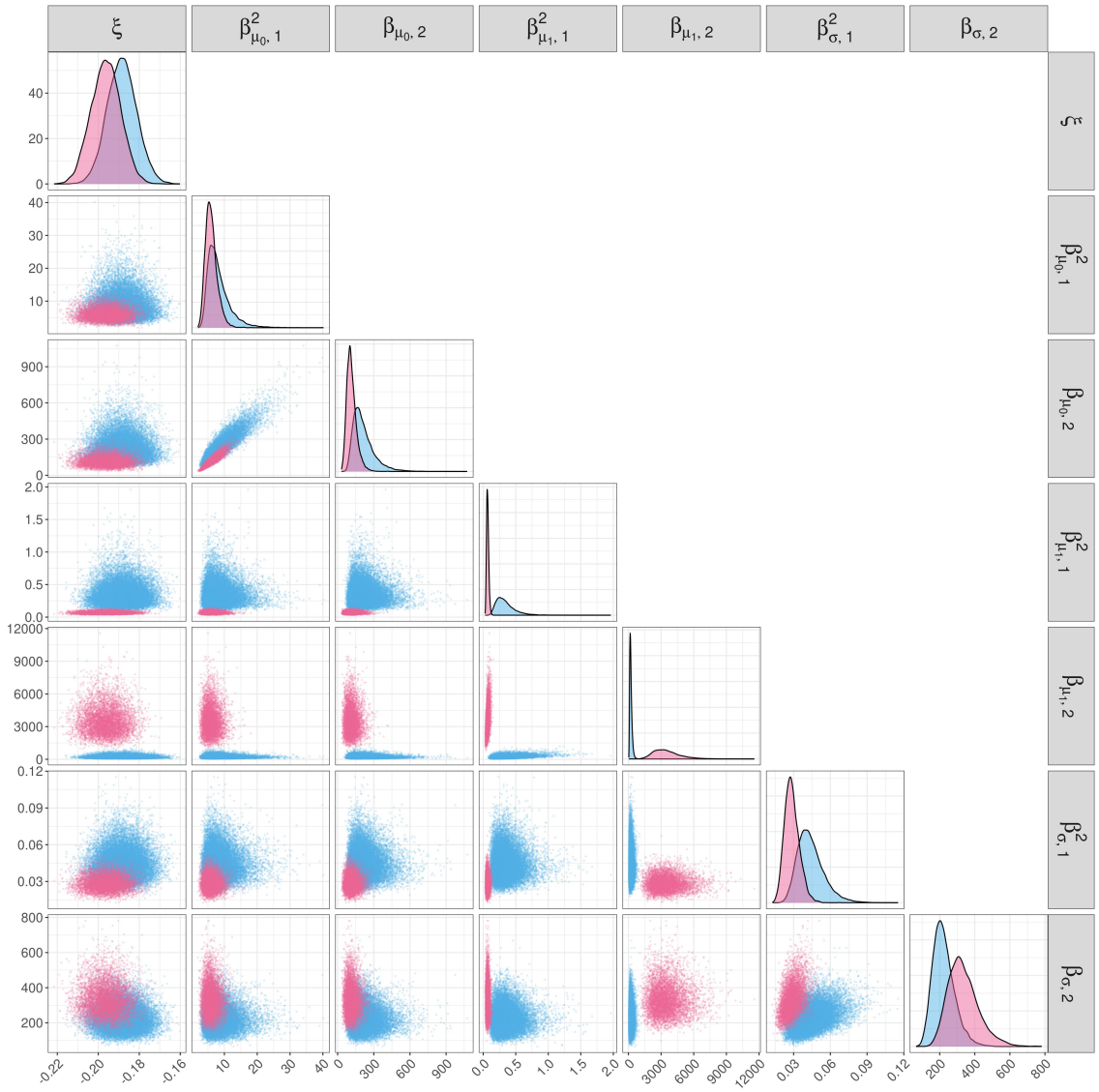


Figure S2: Pairwise posterior distributions of the spatial covariance hyperparameters (Eq. 5) and shape parameter (ξ) for the non-stationary spatial GEVD model of summer TXx, comparing draws obtained via MCMC (blue) and the Laplace approximation (pink). Diagonal panels show marginal posterior densities; lower-triangle panels show bivariate scatter plots of MCMC and Laplace draws.

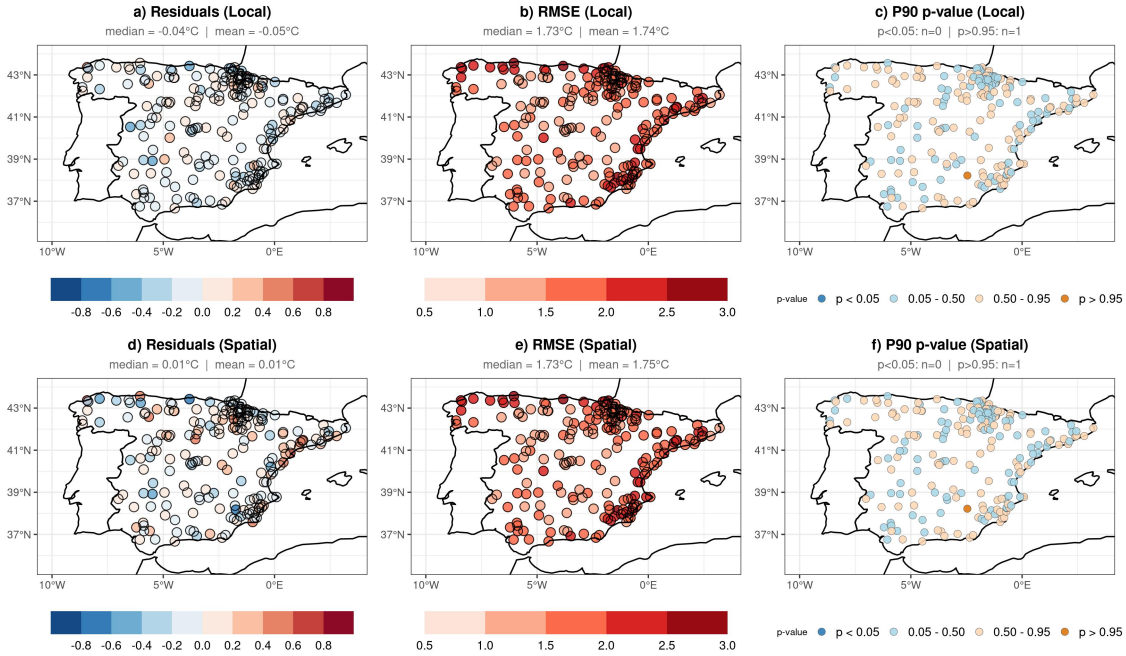


Figure S3: Goodness-of-fit diagnostics for the local (top row, a-c) and spatial (bottom row, d-f) non-stationary GEVD models for summer TXx, based on posterior predictive replicates from MCMC. Left: median posterior residuals (predicted - observed TXx, °C) at each station, with red (blue) colors indicating under- (over-) prediction (a, d). Center: root-mean-square error (RMSE, °C) between observed and posterior predictive mean TXx (b, e). Right: posterior predictive p-value for the 90th percentile of TXx, categorized as p < 0.05 (model underpredicts), 0.05–0.50 and 0.50–0.95 (well calibrated), and p > 0.95 (model overpredicts); station counts falling outside the calibrated range (0.05–0.95) are given above each panel (c, f).

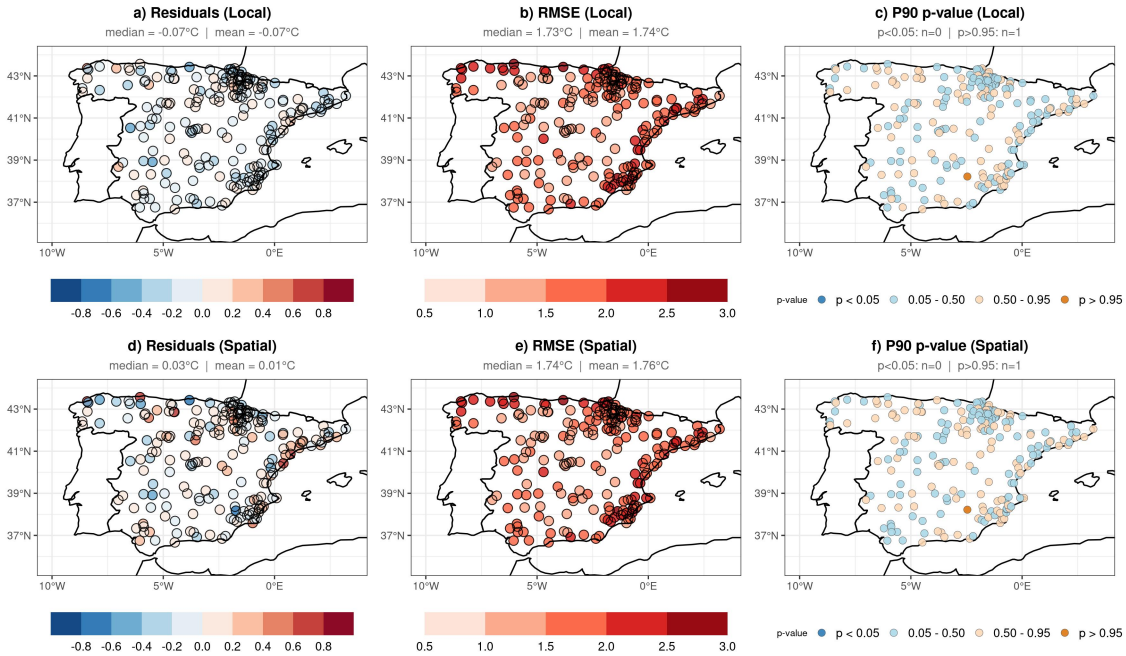


Figure S4: Same as Fig. S3 but using the Laplace approximation.

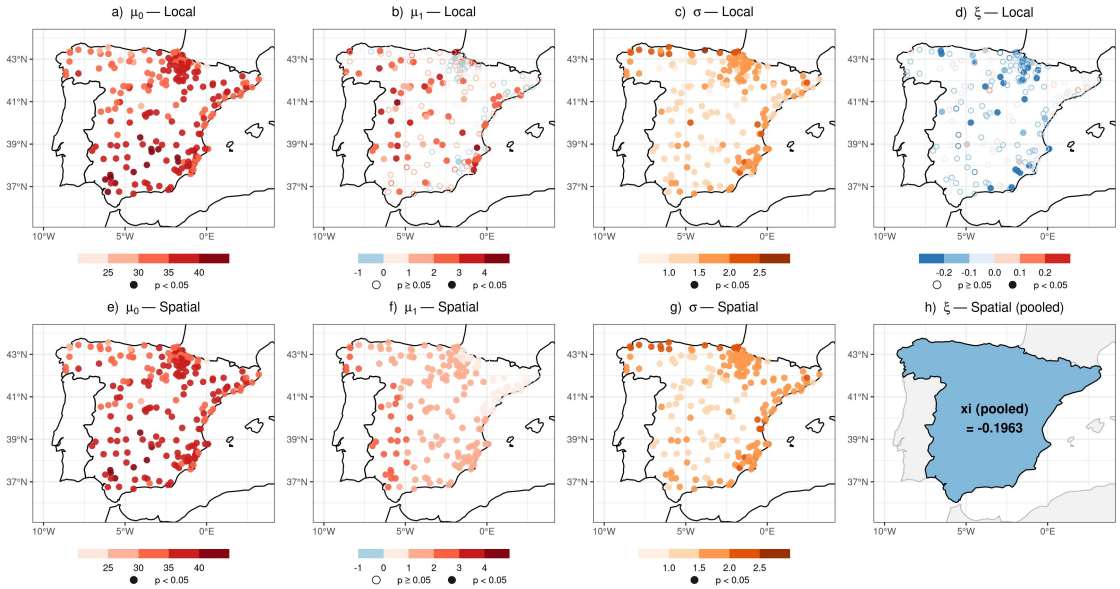


Figure S5: Same as Fig. 3 of the main text but for the Laplace approximation.

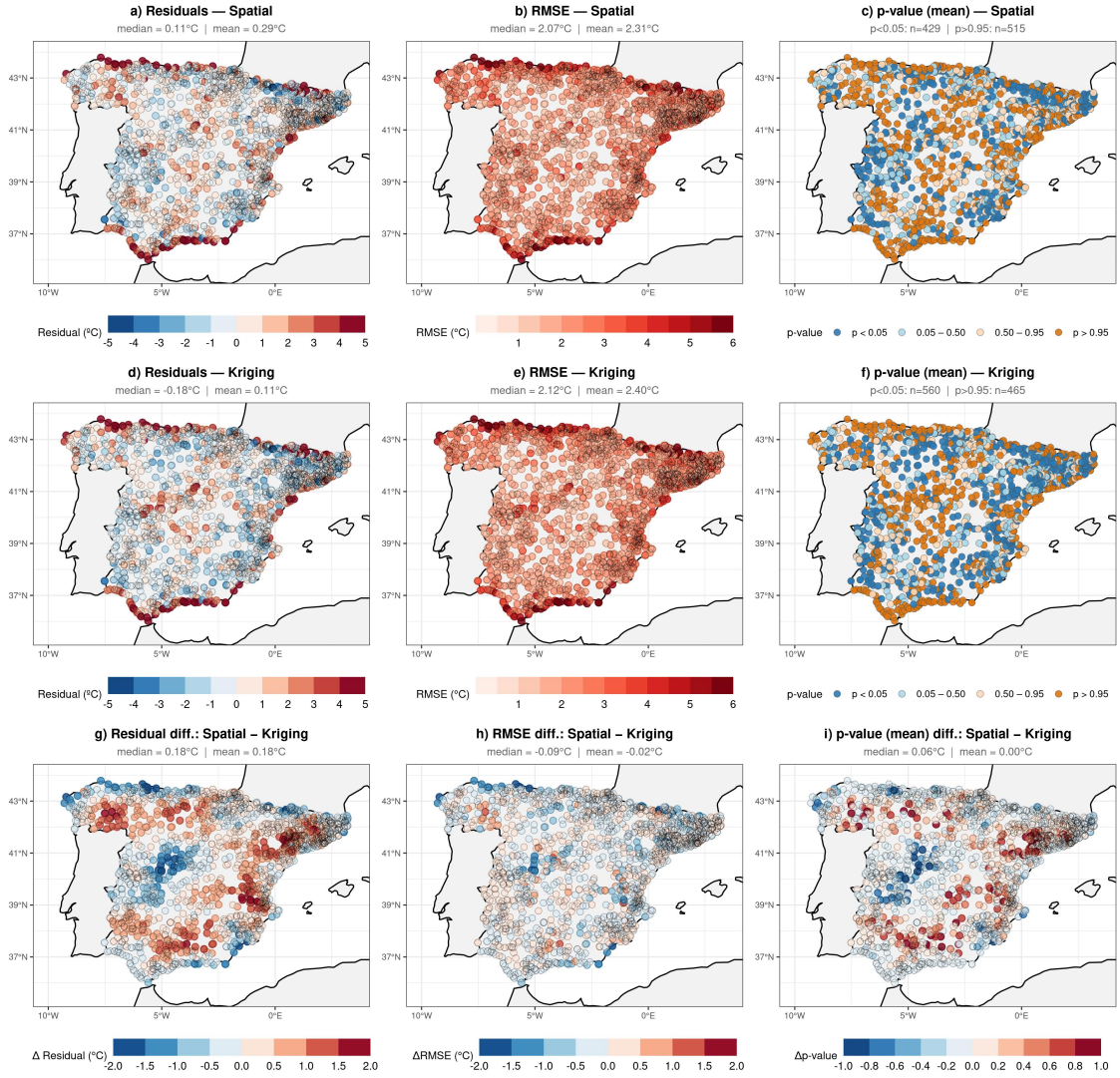


Figure S6: Same as Fig. 4 of the main text but for the Laplace approximation.

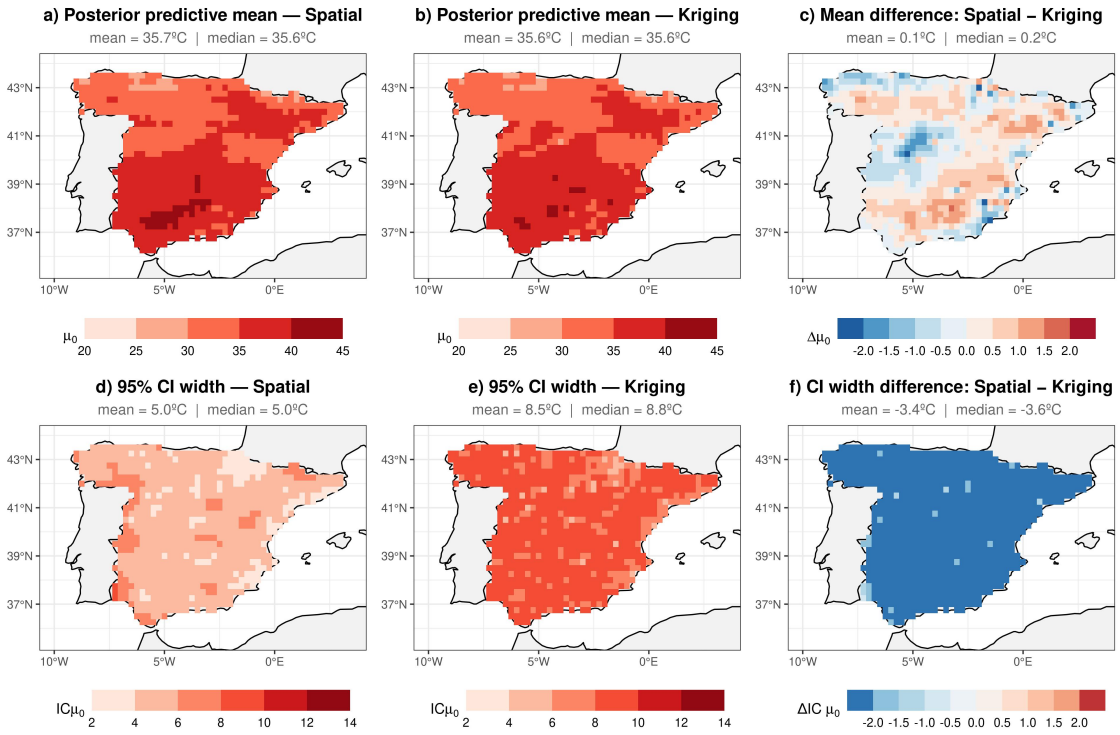


Figure S7: Posterior predictive estimates of the location intercept (μ_0, a-c) and the 95% CI (d-f) for two modeling approaches of summer TXx: a fully Bayesian spatial model using MCMC (a, d) and a kriging-based interpolation (b, e), and their differences (c, f).

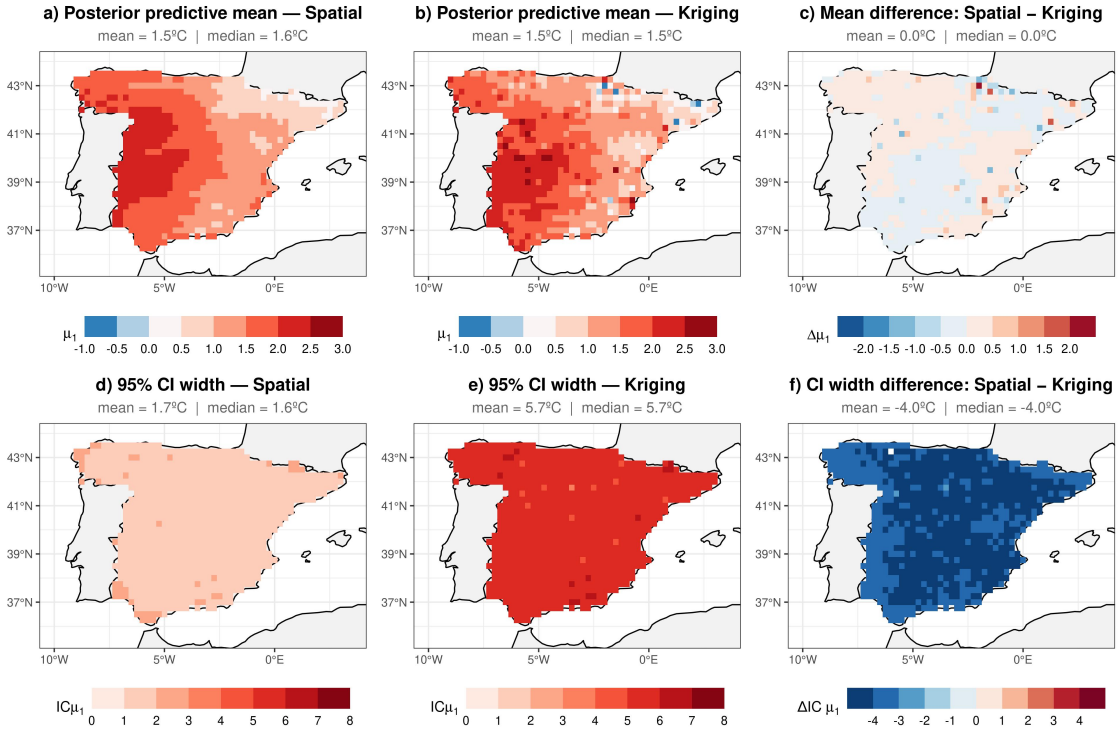


Figure S8: Same as Fig. S7 for the location slope (μ1).

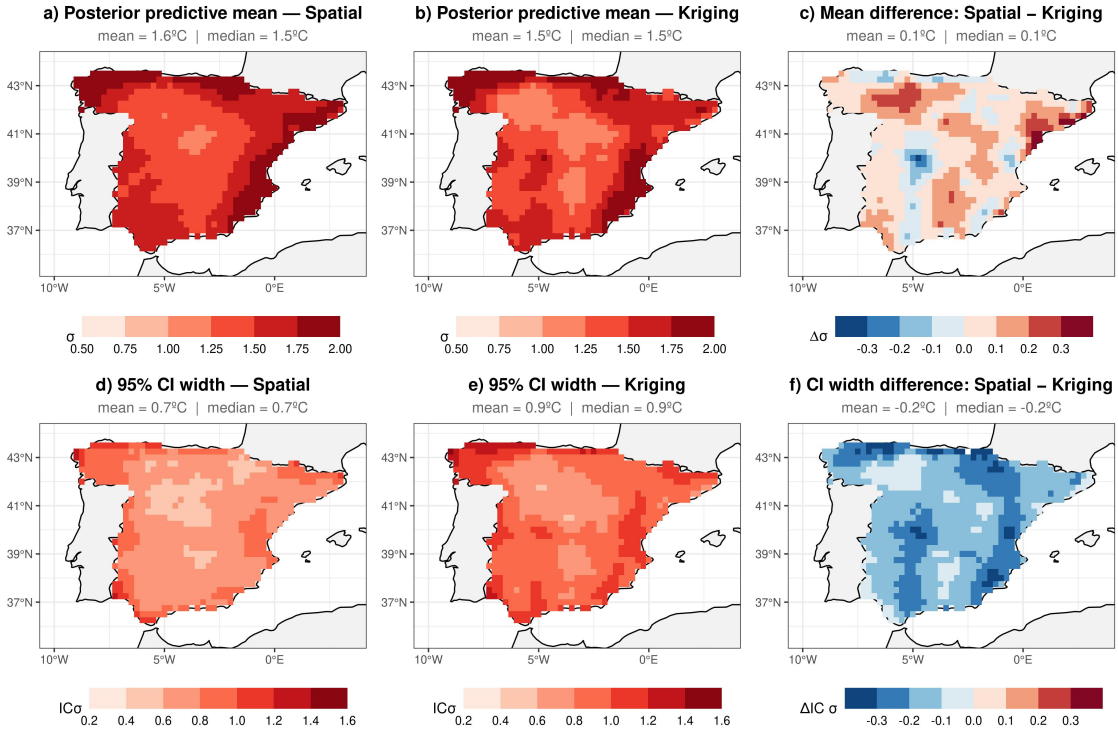


Figure S9: Same as Fig. S7 for the scale parameter (σ).

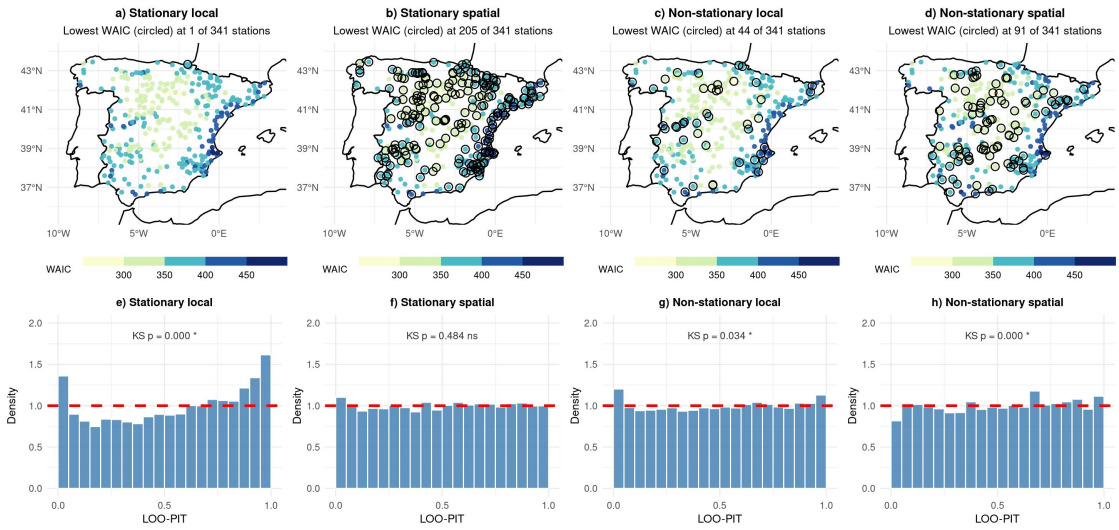


Figure S10: Same as Fig. S1 but for autumn extreme precipitation (Rx1day).

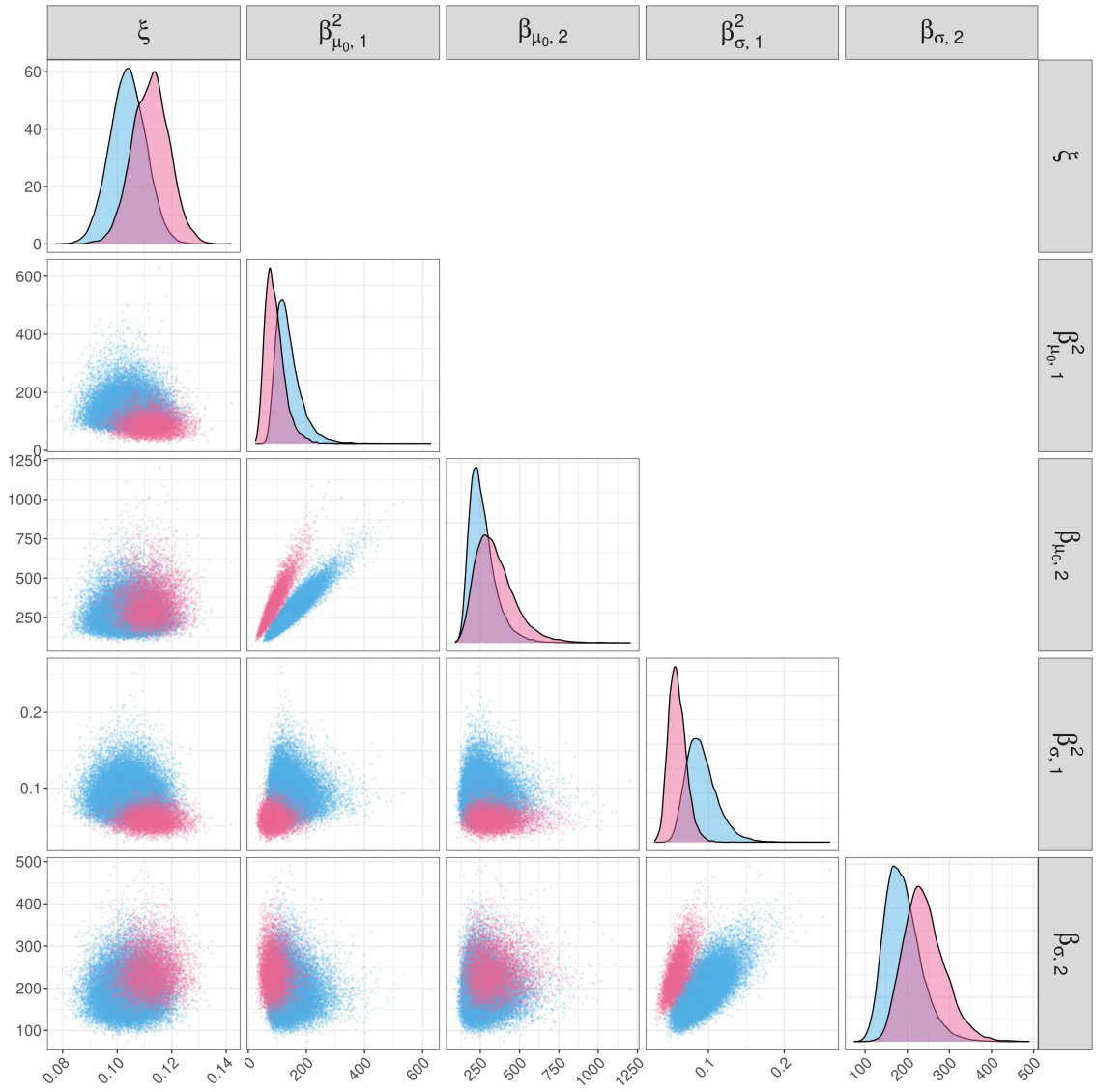


Figure S11. Same as Fig. S2, but for the stationary spatial GEVD model fitted to autumn extreme precipitation (Rx1day).

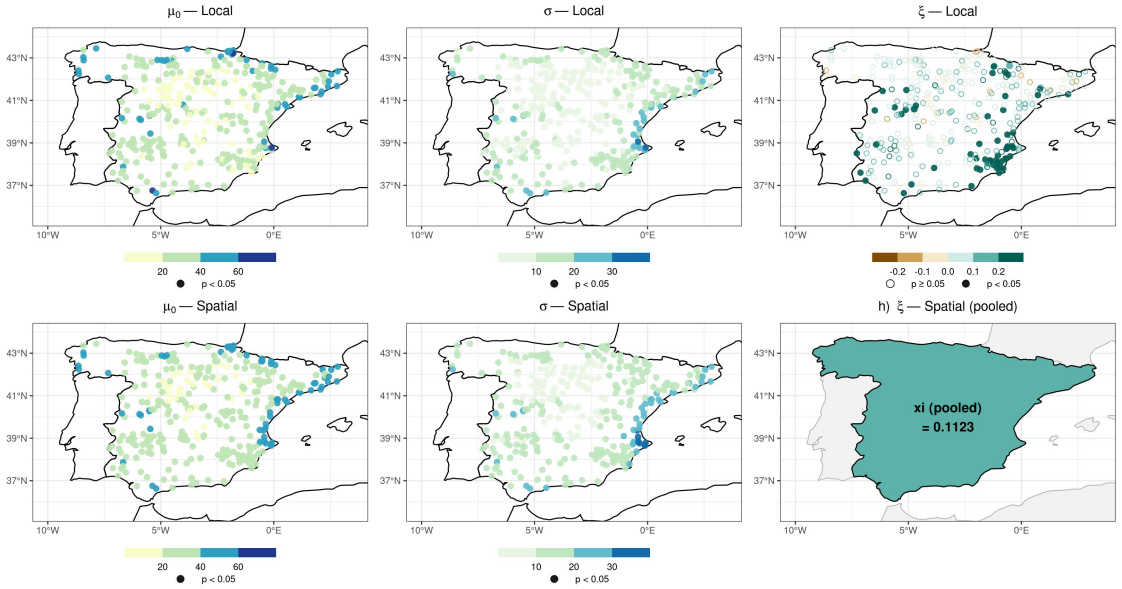


Figure S12: As Fig. 7 of the main text but for the Laplace approximation.

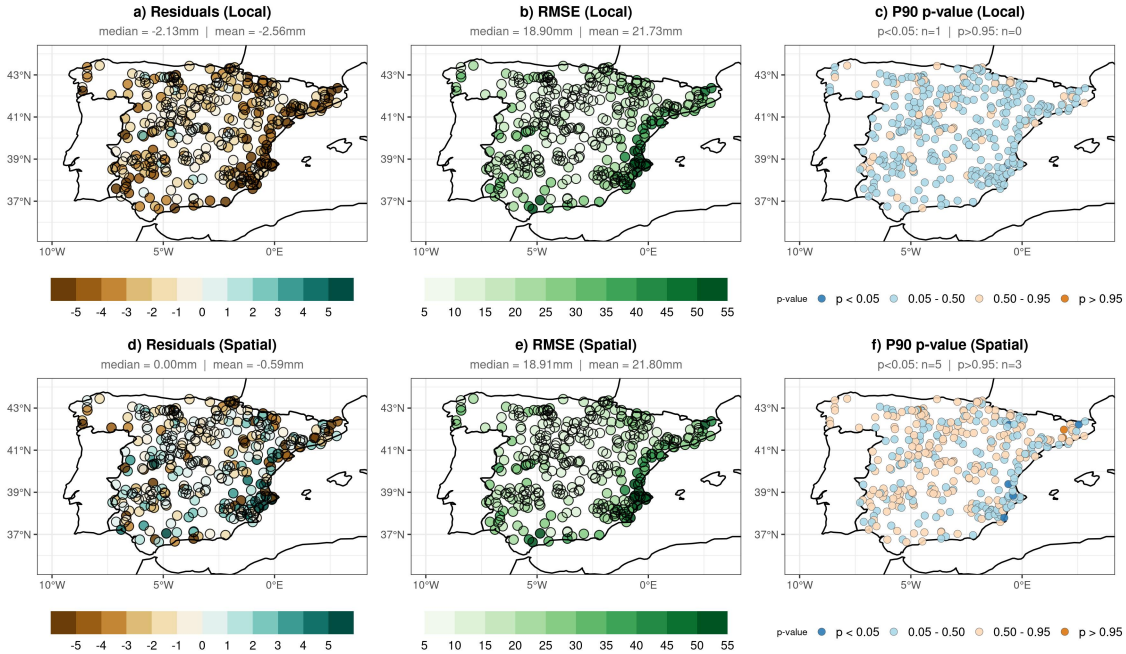


Figure S13: As Fig. S3 but for autumn Rx1day.

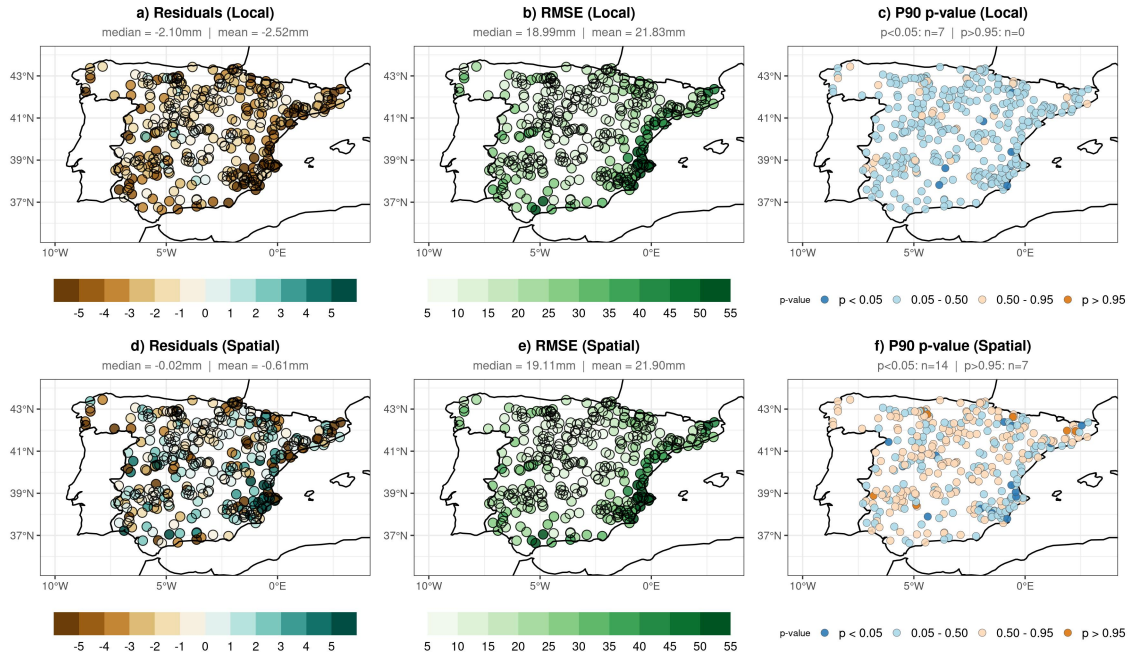


Figure S14: Same as Fig. S13 but using the Laplace approximation.

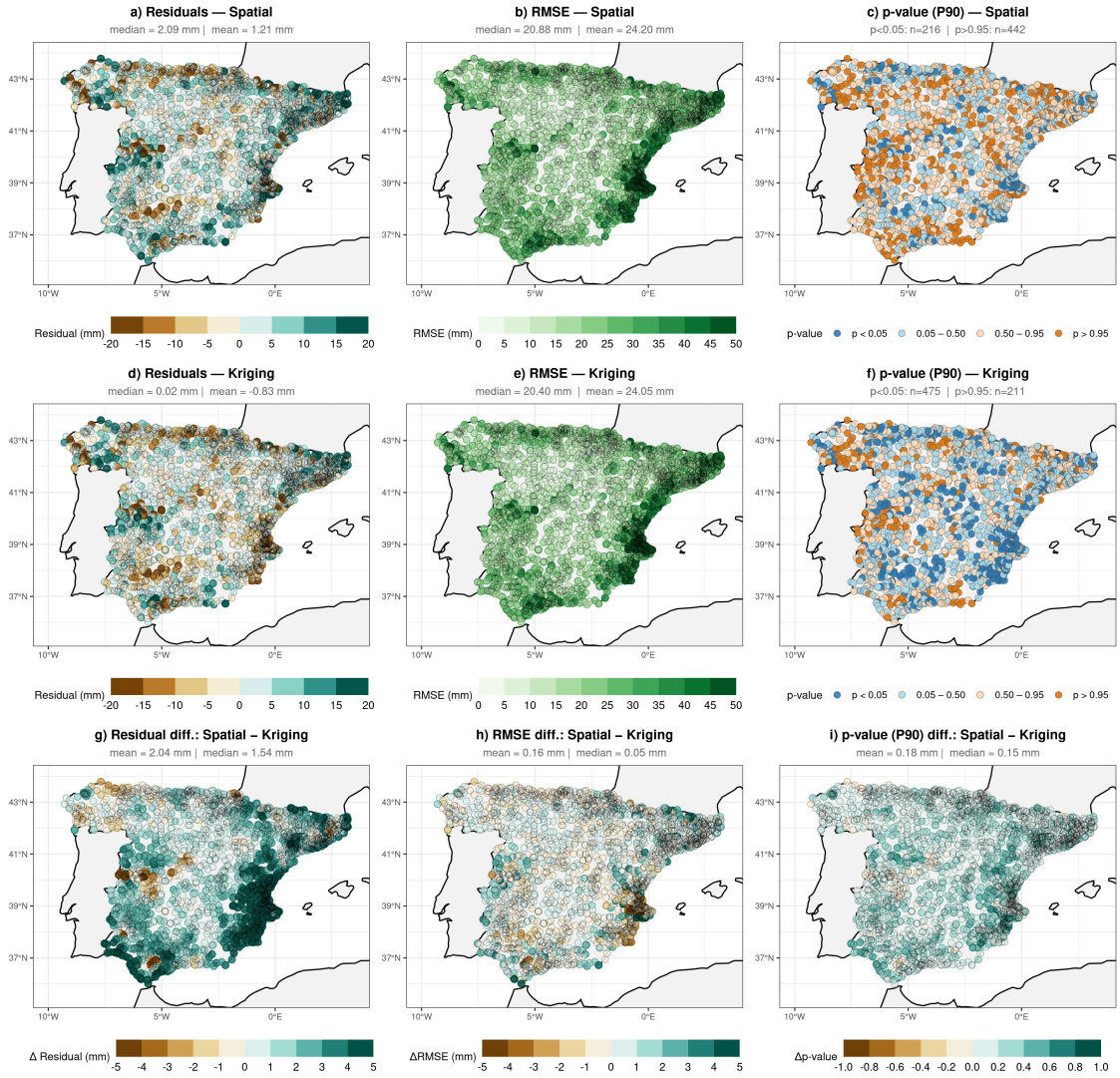


Figure S15: As Fig. 8 of the main text bur for the Laplace approximation.

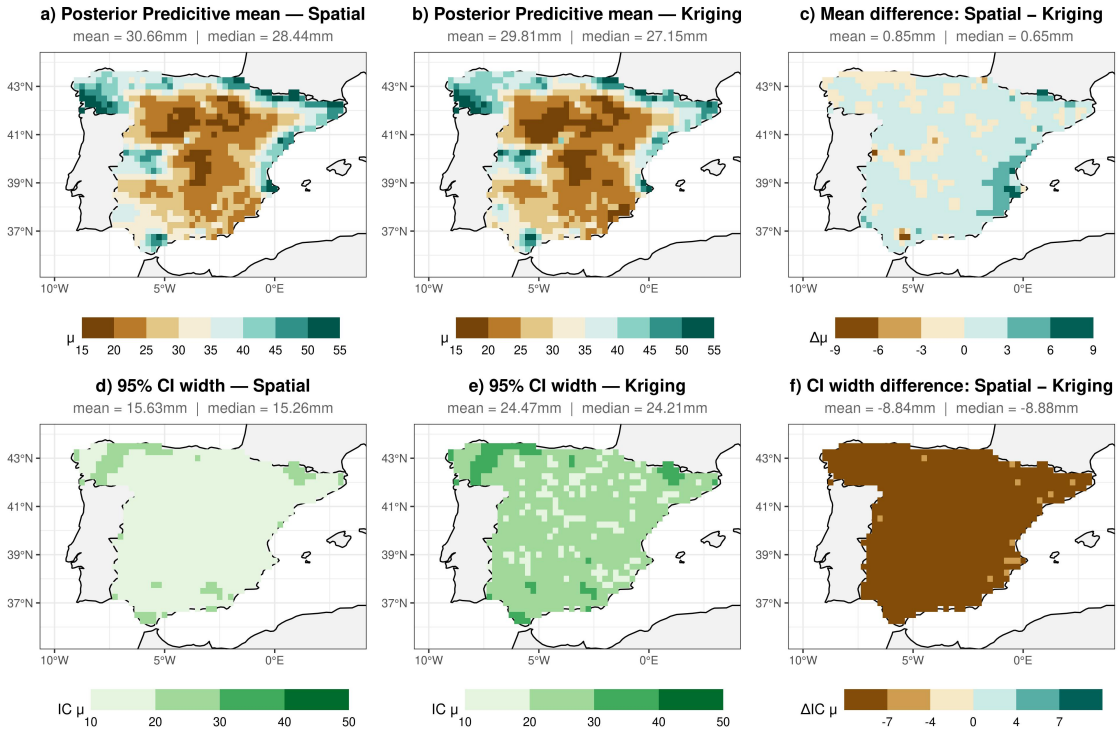


Figure S16: As Fig. S7 but for autumn Rx1day.

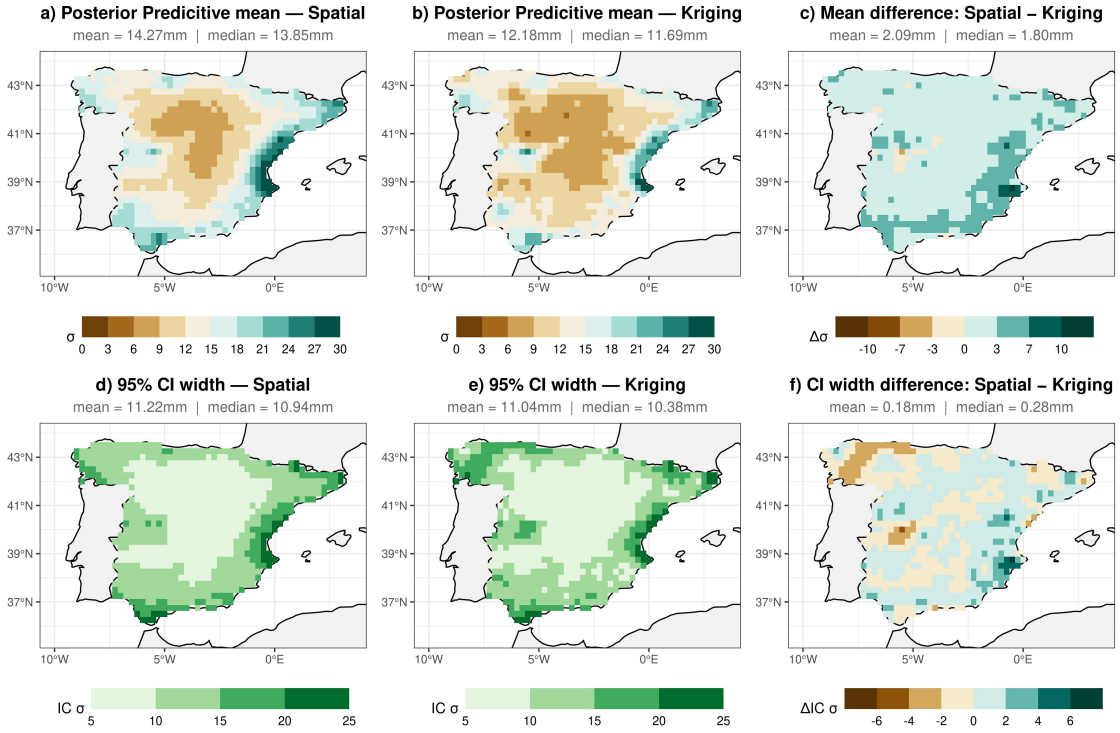


Figure S17: Same as Fig. S16 for the scale parameter (σ).

Supplementary Tables

Variable	*Model*	*Laplace approximation*	*MCMC sampling*
TXx	*full Bayesian non-stationary spatial model*	*173.7 s*	*160511.8 s (~2 days)*
Rx1day	*full Bayesian stationary spatial model*	*352.8 s*	*1093610 s (~13 days)*

Table S1: Execution time (in seconds) required to fit the fully Bayesian spatial model for summer TXx and autumn Rx1day using the Laplace approximation and MCMC sampling, executed from an RStudio Server session on a HPC server, without GPU acceleration. Reported times are hardware- and configuration-dependent and are intended to illustrate the relative computational cost of the two inference approaches rather than to serve as an absolute benchmark.

Parameter	Intercept	Elevation (km)	Longitude (°)	Latitude (°)	Coast distance (km)
μ_0 ($°C$)	**59.59 (36.95; 82.97)**	**-4.63 (-5.53; -3.69)**	0.17 (-0.21; 0.55)	**-0.66 (-1.21; -0.12)**	**0.03 (0.02; 0.04)**
μ_1 ($°C$ / $°C$)	**6.31 (2.42; 10.25)**	-0.29 (-0.77; 0.19)	**-0.15 (-0.22; -0.07)**	-0.08 (-0.17; 0.02)	0.0017 (-0.0003; 0.0038) (
σ ($°C$)	-0.76 (-2.96; 1.35)	-0.07 (-0.16; 0.02)	-0.009 (-0.046; 0.027)	0.04 (-0.01; 0.09)	**-0.0011 (-0.0018; -0.0003)**

Table S2: Same as Table 1 of the main text but for the Laplace approximation.

Parameter	Intercept	Elevation (km)	Longitude (°)	Latitude (°)	Coast distance (km)
μ_0 (mm)	3.51 (-61.80; 86.50)	**7.16 (4.88; 9.37)**	-0.06 (-1.28; 1.18)	0.58 (-1.36; 2.47)	**-0.06 (-0.09; -0.04)**
σ (mm)	**3.67 (0.86; 6.48)**	**7.16 (4.88; 9.37)**	-0.002 (-0.041; 0.038)	0.005 (-0.012; 0.022)	**-0.02 (-0.03; 0.01)**

Table S3: Same as Table 2 of the main text but for the Laplace approximation.